

This is an electronic reprint of the original article. This reprint may differ from the original in pagination and typographic detail.

Brønsted acid catalyzed Prins-Ritter reaction for selective synthesis of terpenoid-derived 4-amidotetrahydropyran compounds

Sidorenko, A. Yu; Kurban, Yu M.; Peixoto, A. F.; Li-Zhulanov, N. S.; Sánchez-Velandia, J. E.; Aho, A.; Wärnå, J.; Gu, Y.; Volcho, K. P.; Salakhutdinov, N. F.; Murzin, D. Yu; Agabekov, V. E.

Published in:
Applied Catalysis A: General

DOI:
[10.1016/j.apcata.2022.118967](https://doi.org/10.1016/j.apcata.2022.118967)

Published: 05/01/2023

Document Version
Final published version

Document License
CC BY

[Link to publication](#)

Please cite the original version:

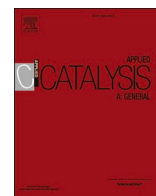
Sidorenko, A. Y., Kurban, Y. M., Peixoto, A. F., Li-Zhulanov, N. S., Sánchez-Velandia, J. E., Aho, A., Wärnå, J., Gu, Y., Volcho, K. P., Salakhutdinov, N. F., Murzin, D. Y., & Agabekov, V. E. (2023). Brønsted acid catalyzed Prins-Ritter reaction for selective synthesis of terpenoid-derived 4-amidotetrahydropyran compounds. *Applied Catalysis A: General*, 649, Article 118967. <https://doi.org/10.1016/j.apcata.2022.118967>

General rights

Copyright and moral rights for the publications made accessible in the public portal are retained by the authors and/or other copyright owners and it is a condition of accessing publications that users recognise and abide by the legal requirements associated with these rights.

Take down policy

If you believe that this document breaches copyright please contact us providing details, and we will remove access to the work immediately and investigate your claim.



Brønsted acid catalyzed Prins-Ritter reaction for selective synthesis of terpenoid-derived 4-amidotetrahydropyran compounds

A.Yu. Sidorenko^{a,*}, Yu.M. Kurban^a, A.F. Peixoto^b, N.S. Li-Zhulanov^c, J.E. Sánchez-Velandia^d, A. Aho^e, J. Wärnå^e, Y. Gu^f, K.P. Volcho^c, N.F. Salakhutdinov^c, D.Yu. Murzin^{e,*}, V.E. Agabekov^a

^a Institute of Chemistry of New Materials of National Academy of Sciences of Belarus, Skaryna str, 36, Minsk, 220141, Belarus

^b LAQV-REQUIMTE, Departamento de Química e Bioquímica, Faculdade de Ciências, Universidade do Porto, Rua do Campo Alegre s/n, Porto, 4169-007, Portugal

^c Novosibirsk Institute of Organic Chemistry, Lavrentjev av. 9, Novosibirsk, 630090, Russian Federation

^d Sustainable and supramolecular research group, Departamento de Química Inorgánica y Orgánica, Universidad Jaume I, Av. Sos Baynat s/n, Castellón, Castellón, 12071, Spain

^e Åbo Akademi University, Henriksgatan 2, 20500 Turku/Åbo, Finland

^f Huazhong University of Science and Technology, 103 7 Luoyu Road, Hongshan District, Wuhan 430074, China

ARTICLE INFO

Keywords:

Prins-Ritter
SO₃H-functionalized solids
(-)-isopulegol
benzaldehyde
DFT
Kinetic modelling

ABSTRACT

A number of SO₃H-functionalized solids (biochar, montmorillonites, carbon and halloysite nanotubes) has been studied as catalysts in the cascade Prins-Ritter reaction of (-)-isopulegol with benzaldehyde and acetonitrile for synthesis of octahydro-2H-chromene amides (as 4R- and 4S-isomers). A high selectivity to these products at 30 °C in the presence of H₂O was observed on catalysts modified with chlorosulfonic acid (CSA) reaching 84% (4R/4S of 5.7) in the case of biochar, while a relatively large amount of octahydro-2H-chromenols (up to 31%), products of Prins condensation, was formed on the materials functionalized by 2-(4-chlorosulfonylphenyl)ethyltrimethoxysilane (CSP). Although Prins condensation proceeds efficiently on weak acid sites, the Prins-Ritter reaction requires sulfated materials with strong (0.33 – 5.8 mmol/g) Brønsted acidity. Catalysts functionalized by CSP were stable, while for the materials modified with chlorosulfonic acid, leaching of -SO₃H groups was observed. Nonetheless, on resistant Biochar-CSP, selectivity to the amides at 30 °C (67%) was higher than that with the commercial Amberlyst-15 (47%), and triflic acid at – 25 °C (62%). Similar selectivity to the desired products on Biochar-CSA (-SO₃H groups) and H₂SO₄ (81–84%) as well as on Biochar-CSP (-PhSO₃H) and with *p*-toluenesulfonic acid (67–70%) was observed. DFT calculations and experimental results showed that at 30 °C formation of 4S-amide thermodynamically is more beneficial than of alcohols and dehydration products. However, addition of water results in a sharp increase in the reaction rate and 4R-amide selectivity due to a change to the kinetic control, leading eventually to both high yields and stereoselectivity. The proposed reaction pathways also were confirmed by kinetic modelling.

1. Introduction

The amide moiety is present in various functional molecules, for example bioactive compounds, clinically approved drugs, DNA damage probes, precursors of liquid crystal polymers, etc. [1–3]. An effective method of amide synthesis is the Ritter reaction, which involves interactions of alcohols or alkenes with nitriles in the presence of acid catalysts [2,4]. Utilization of this reaction in the tandem (cascade) fashion is under intensive development making it possible to realize

formation of several chemical bonds in one reactor space without separating intermediates [2,4–6].

When unsaturated alcohols, aldehydes and nitriles in the presence of catalysts undergo a tandem three-component Prins-Ritter reaction, products with a 4-amidotetrahydropyran fragment are formed as illustrated in Fig. 1 [2,7,8]. It is well-known from the literature that such compounds can exhibit a wide spectrum of biological activity [2,9–11].

To carry out the Prins-Ritter reaction, homogeneous catalysts are usually used, in particular, BF₃·Et₂O [7,11–13], HBF₄·Et₂O [14], TfOH

* Corresponding authors.

E-mail addresses: sidorenko@ichnm.by (A.Yu. Sidorenko), dmurzin@abo.fi (D.Yu. Murzin).

<https://doi.org/10.1016/j.apcata.2022.118967>

Received 5 September 2022; Received in revised form 11 November 2022; Accepted 13 November 2022

Available online 21 November 2022

0926-860X/© 2022 The Author(s). Published by Elsevier B.V. This is an open access article under the CC BY license (<http://creativecommons.org/licenses/by/4.0/>).

[8,15], TMSOTf [16], Bi(OTf)₃ [17], *o*-benzenedisulfonimide [18], B(C₆F₅)₃ [19], Ce(SO₄)₂ [20] or some binary systems such as CeCl₃·7 H₂O/AcCl [21], I₂/AcCl [22] and TMSOTf/TfOH [23]. Synthesis is most often performed at temperatures ranging from – 50–0 °C [8, 14,15,19,23] in an excess of the corresponding nitrile (both as a solvent and a reagent) [8,13,14,17,22] or in methylene chloride [8,14,23]. It should be noted that the results of these studies are presented mainly in the context of synthetic organic or medicinal chemistry without considering the effect of the catalyst either homogeneous or heterogeneous.

One of the topical areas of green chemistry is the use of renewable raw materials in cascade transformations for the efficient synthesis of chemical products [24]. In this context, the natural terpenoid (–)-isopulegol is a suitable chiral platform for the synthesis of a wide range of biologically active compounds [25], which, in particular, exhibit high analgesic [26] and antiviral [27] activity. It has recently been shown, that (–)-isopulegol derivatives with an octahydro-2*H*-chromene structure containing the amide fragments are potent inhibitors of the TDP1 enzyme being promising in the complex anticancer therapy [28]. Moreover, several amides derived from terpenoids exhibit high antitumor [29,30], antiviral [31,32], antioxidant [33] and other bioactivities [31].

According to a literature report [8], synthesis of isopulegol-derived 4-amidotetrahydropyran compounds can be carried out in the presence of 2–3 equivalents of triflic acid (TfOH) in the temperature range from – 50 to – 25 °C, because under ambient conditions a multicomponent mixture is formed. Considering that octahydro-2*H*-chromene amides can have a significant pharmaceutical potential, development of active and selective heterogeneous catalysts exhibiting high yields and able to operate at ambient conditions is highly desirable.

Aluminosilicates (in particular, montmorillonite and halloysite) [34, 35], as well as carbon [36] materials, are a promising basis for such novel catalytic systems due to their availability, possibility of functionalization, and, what is important in the context of medicinal chemistry, low toxicity [34–36].

Until recently, heterogeneous catalysts for the tandem Prins-Ritter reaction have not been reported [37], although it is known that modified clays [15,38,39], halloysite nanotubes [40,41], hierarchical zeolites [42,43], Cs_{2.5}H_{0.5}PW₁₂O₄₀ [44] are efficient catalytic systems for the Prins [15,38,40,41,44] and Prins-Friedel-Crafts [39,42–44] reactions.

One of the methods for acid functionalization of solid materials is grafting of –SO₃H groups on their surfaces, allowing preparation of efficient catalysts for various reactions [45,46], in particular, etherification [47], isomerization [48], condensation [38], etc. Therefore, the

materials containing such groups may be promising for acid-catalyzed cascade reactions.

In the previous work [37], the authors have studied for the first time SO₃H-functionalized materials, including carbon nanotubes and K10 clay, as catalysts for the Prins-Ritter reaction involving (–)-isopulegol (Fig. 1b) under mild (30 °C) conditions. A strong effect of water on selectivity was reported, namely addition of water not only sharply increases the overall selectivity to 4-amido-octahydro-2*H*-chromene, but also the yield of the 4*R*-stereoisomer, while the 4*S*-isomer formation is dominated at the minimum amount of added water (Fig. S1, Supplementary Information). Experimental data and DFT calculations clearly indicated the kinetic control for 4*R*-amide formation, whereas 4*S*-amide is formed as a result of the thermodynamic control.

In the preliminary communication, [37] there was no detailed information on the effect of the type and properties of the material used or the impact of functionalization and reaction conditions on selectivity and activity as well as on the leaching of functional groups.

To fill these clear voids, this work is, therefore, devoted to a detailed study of a number of aluminosilicates and carbon materials functionalized with –SO₃H groups in the Prins-Ritter reaction involving (–)-isopulegol (Fig. 1b), covering variations of reaction conditions, DFT calculations, kinetic modelling, and leaching testing. The main attention was paid to the biochar as the support, because it is an affordable biomass waste processing product, in this particular case it was obtained from Portuguese vineyard pruning waste [47]. For better understanding of the reaction, a number of homogeneous Brønsted acids were used and the reaction scope was also examined.

Thus, the main goals of the current work were (i) to develop efficient catalytic procedures for the Prins-Ritter reaction under ambient conditions, (ii) to establish the effect of various catalysts, methods of their modification, and reaction conditions on the yields of the target products, and finally (iii) to elucidate the reaction mechanism and various reaction pathways.

2. Experimental

2.1. Materials and reagents

All reagents and materials were purchased from commercial suppliers and used without any additional chemical treatment unless otherwise stated. For preparation of the biochar, the waste from the pruning of vineyards of the *Vitis vinifera* Tinta Roriz variety (from the Quinta Dos Carvalhais farm, Dao region, Portugal) was used. Before utilization, these wastes were dried for 24 h at 50 °C and crushed to the

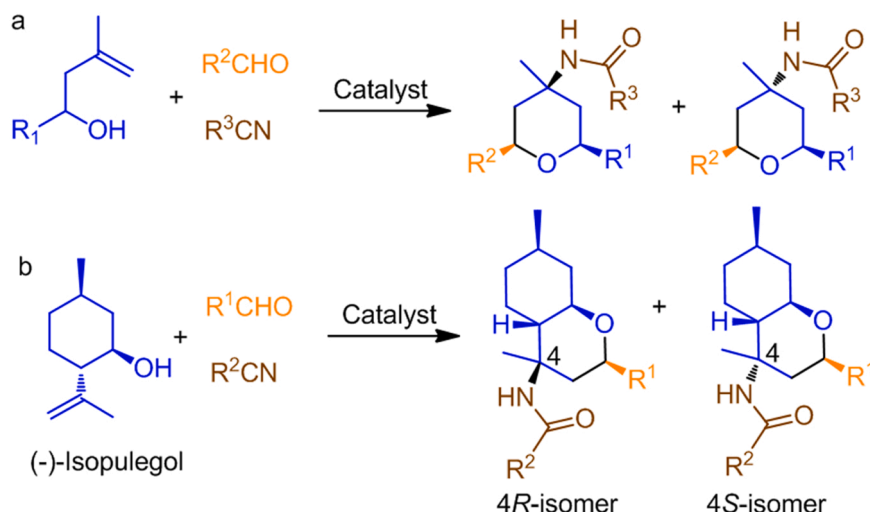


Fig. 1. Examples of the Prins-Ritter tandem reaction involving aliphatic (a) and terpene (b) unsaturated alcohols.

size between 100 and 200 μm .

2.2. Preparation, functionalization and characterization of catalysts

Biochar was produced by hydrothermal carbonization of biomass using a high-pressure batch reactor of Parr Instrument Co. For this purpose, 40 g of the vineyard pruning waste and 400 mL of deionized water were placed in a 500 mL vessel, heated with continuous stirring to 250 °C (autogenous pressure of 45–50 bar), and treated for 50 min under these conditions. The solid phase was removed from the reactor, dried at 100 °C overnight and then activated CO_2 at 800 °C for 30 min in flow which is a typical procedure for pore enlargement [47].

The prepared biochar (BioC) was functionalized with chlorosulfonic acid (i), 2-(4-chlorosulfonylphenyl)ethyltrimethoxysilane (ii), and H_2SO_4 (iii) according to the procedures described in [47]:

(i). In a 50 mL round-bottom flask 30 mL of CHCl_3 , 1.0 g of BioC were added, then 1.0 mL of ClSO_3H (CSA) ($\geq 98\%$, Fluka) was poured dropwise with vigorous stirring and the treatment was carried out at 65 °C for 2 h. The functionalized material (designated as BioC-CSA) was separated from the liquid phase on a filter, washed with CHCl_3 , methanol and dried at 100 °C for 24 h.

(ii). A portion of biochar (2.0 g) was dispersed in 100 mL of anhydrous toluene, then 1.84 mL (7.8 mmol, 50% solution in CH_2Cl_2) of 2-(4-chlorosulfonylphenyl)ethyltrimethoxysilane (CSP) (from ABCR GmbH) was added to the resulting suspension with stirring and functionalization was carried out for 24 h at 110 °C in an inert atmosphere. Then, the resulting material (BioC-CSP) was separated by centrifugation, washed with 100 mL of toluene, filtered and dried (100 °C, 24 h).

(iii). In a 50 mL round-bottom flask 1.0 g of biochar and 20 mL of 95.0% sulfuric acid (95%, VWR Chemicals) were placed with constant stirring at 80 °C for 6.0 h. The final product (BioC- H_2SO_4) was separated from the liquid phase, washed with distilled water until pH > 6, and dried at 100 °C for 24 h.

Commercial montmorillonites K10 (Acros Organics), Na-CLOI (Southern Clay) and halloysite nanotubes (HNT, Sigma-Aldrich) were functionalized with chlorosulfonic acid and 2-(4-chlorosulfonylphenyl)ethyltrimethoxysilane according to procedures similar to those described above, however, in the case of CSA, the treatment was carried out at room temperature [38]. Carbon nanotubes (CNT, Nanocyl S.A., >95% purity) were oxidized with 7.0 M HNO_3 at 80 °C for 3 h (ox-CNT) and then treated with a solution of CSP (CNT-CSP) in dry toluene according to the procedure described in [37].

Functionalization of carbon and aluminosilicate materials is schematically illustrated in Fig. 2. The resulting catalysts were characterized in detail by several physico-chemical methods including XRD, EA, XPS, TG, N_2 adsorption-desorption, SEM and FTIR as described in [37,38,45]. Acidity of the samples was determined by the potentiometric back titration [38,47] and FTIR spectroscopy using pyridine as a probe molecule in the case of clays [38]. The latter method was applied in the

present study to evaluate the concentration of acid sites (a.s.) in the catalysts before and after the reaction. Detailed descriptions of the catalyst characterization procedures are given in SI.

2.3. Reaction and products analysis

A typical experiment was performed as follows according to the previous work [37]. To a three-necked flask 50 mL 0.1 g (0.65 mmol) of (-)-isopulegol ($\geq 98\%$, Sigma-Aldrich), 0.32 g (3.0 mmol) of benzaldehyde, 0.31 g (17.3 mmol) of distilled water and 0.1 g of undecane (the internal standard, 99%, Merck) were added. Acetonitrile (99.9%, extra dry, Acros Organics) was used both as a solvent and a reagent; the total volume of the mixture was 20 mL. After heating to 30 °C, 0.1 g of the catalyst (dried for 2 h at 110 °C, particle size <100 μm) was added to the reactor and stirring was started using a magnetic stirrer (300 rpm) to avoid both internal and external mass transfer limitations [37,39,41]. Samples of the reaction mixture (150 μL) were periodically taken for analysis. Altogether six samples were withdrawn from the mixture. The reaction has also been studied at temperatures from 15° to 35 °C and an initial concentration of isopulegol from 0.013 to 0.13 mol/L. The equations for calculating the initial consumption rate of (-)-isopulegol, its conversion and selectivity are given in the SI.

In the case of using homogeneous catalysts (1.0 eq), the reaction was carried out in a round bottom flask (50 mL) at 25 °C for 3 h, thereafter the mixture was evaporated on a rotary evaporator and neutralized with the saturated sodium bicarbonate solution (10 mL), which was followed by extraction of the reaction products with ethyl acetate (10 mL).

The reaction mixture was analyzed by gas chromatography using a Khromos GC-1000 chromatograph with a Zebron ZB-5 capillary column (30 m x 0.25 mm x 0.25 μm) and a flame ionization detector. The temperature of the evaporator and detector were 250 and 280 °C, respectively. The column heating from 110° to 280 °C was realized at a ramping rate of 20 °C/min, followed by the isothermal mode. The total analysis time was 25 min. A typical chromatogram of the reaction products is shown in Fig. S2.

2.4. DFT calculations

The optimization of the structures was performed at the DFT level using the hybrid functional of the electronic density B3LYP (considering computational costs, accuracy and coverage of the result, as it was reported previously) with the 6-311 + +g(d,p) basis set [49]. All computational runs were carried out in the Gaussian09 program. Typical DFT methods fails to describe the Van der Waals interactions which are of non-local forces. To improve this deficiency, the empirical dispersion correction of Grimme (D3) was considered during both optimization and frequencies calculations [50].

The minimal structures were verified with the frequency values (only one positive value) and confirmed by calculating the second derivatives

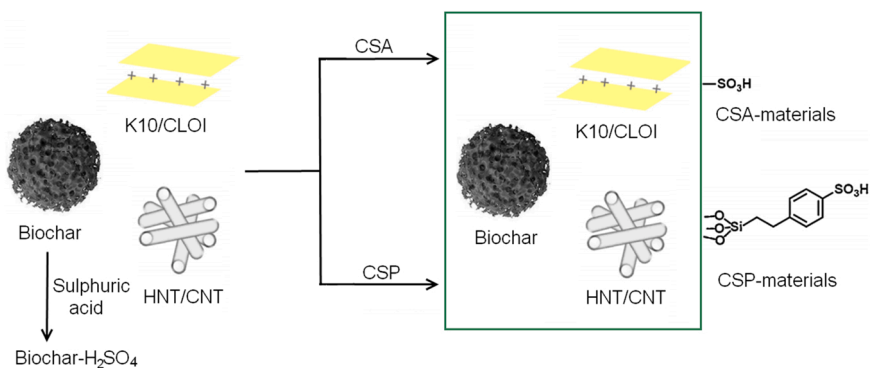


Fig. 2. Schematic illustration of the studied materials functionalization with chlorosulfonic acid (CSA), 2-(4-chlorosulfonylphenyl)ethyltrimethoxysilane (CSP), and H_2SO_4 (Biochar only).

of the energy, which confirm of the nature of the stationary point. Solvation effects (acetonitrile) were included and computed at the same level of theory on the optimized structures by using the conductor-like polarizable continuum model (CPCM) implemented in the GaussianG09 package [51]. The model involves the solute cavity via a set of overlapping spheres, using a continuous surface charge formalism that ensures continuity and robustness of the reaction. The initial reference ($\Delta G=0.0$) was taken as the sum of isopulegol, benzaldehyde, acetonitrile and the homogeneous catalyst (H_2SO_4 or p -TSA).

3. Results and discussion

3.1. Physico-chemical properties of SO_3H -functionalized materials

The investigated solids were thoroughly characterized in the recent works [37,38,40,47], and their main physico-chemical properties are summarized in Table 1. Functionalization of aluminosilicate and carbon materials with chlorosulfonic acid (CSA) and 2-(4-chlorosulfonylphenyl)ethyltrimethoxysilane (CSP) led to a significant decrease in their specific surface area (S_{BET}) and the pore volume (V_{pore}), while acidity of these materials increased as expected, being the largest for K10-CSA. At the same time, an increase in the concentration of Brønsted acid sites was predominantly observed. Note that relatively high S_{BET} values were observed for the initial and modified biochar samples (Table 1).

The presence of sulfur in the functionalized materials was clearly confirmed by EA and XPS analyses (Table 1). Images of scanning electron microscopy (SEM) of the parent and functionalized biochars are shown in Fig. 3, while those for aluminosilicates were given in [38]. When the parent biochar is compared with those modified by both acids, some rugosity with irregular shapes could be observed in addition to open sheets with non-uniform cavities. The acid treatment seems to destroy the geometrical open sheets giving new cavities. In the same way, some crystals are visible when BioC is modified with CSA. It appears that CPS treatment has a larger impact compared with CSA.

3.2. Catalytic activity

3.2.1. Influence of the type and properties of SO_3H -functionalized material

The Prins-Ritter reaction was studied in the presence of 17.3 mmol of added water, since this amount provided both the largest selectivity to the target amides and the highest 4R/4S isomers ratio [37].

In the presence of the initial aluminosilicate and carbon materials

(K10, CLOI, HNT, BioC), the reaction of (-)-isopulegol **1** with benzaldehyde **2** and acetonitrile did not proceed. After their functionalization with SO_3H -groups, the formation of amides of octahydro-2H-chromene **3** (4R- and 4S-diastereomers), as well as octahydro-2H-chromen-4-ols **4** and dehydration compounds **5** was observed (Fig. 4, Table 2). However, after 4 h of the reaction on CLOI-CSP, HNT-CSA, and BioC- H_2SO_4 , conversion of (-)-isopulegol **1** did not exceed ca. 18% (Table 2).

When using CSA-functionalized materials, formation of amides **3** (the Prins-Ritter reaction products) was more pronounced than in the case of solids, modified by CSP, reaching 83.8% with the 4R/4S isomers ratio of 5.7 on BioC-CSA (Table 2, entry 7). Note that selectivity over this catalyst was almost identical to the values obtained for carbon nanotubes modified with chlorosulfonic acid [37] (Table 2, entry 11). Thus, the type and morphology of the starting carbons do not affect their catalytic behavior.

On the other hand, although the total yield of amides **3** on clay (K10, CLOI) and carbon (BioC and CNT) materials, modified with chlorosulfonic acid was comparable (76.2–83.8%, Table 2), the stereoselectivity (i.e. 4R/4S ratio) obtained in the case of aluminosilicates did not exceed 2.4 while on BioC it reached 5.7 (Table 2). For example, the selectivity to 4R-amide on BioC-CSA (71.3%) was significantly higher than in the case of K10-CSA (51.2%).

This can originate from the acid nature of the materials, as on the surfaces of aluminosilicates K10, CLOI, and HNT both Brønsted and Lewis a.s. are present, whereas the carbon materials are practically not acidic (Table 1). As noted above, these parent solids do not exhibit catalytic activity per se. However, it is known that coordination of Lewis a.s. with acids, in particular sulfonic ones, increases their strength [53], which may lead to changes in stereoselectivity for amides **3**.

In the presence of CSP-modified catalyst (i.e. containing $-PhSO_3H$ groups), selectivity to amides **3** did not exceed 73.5% with a rather low (not more than 2.5) value of 4R/4S ratio, while a relatively large amount of alcohols (up to ca. 31% on HNT-CSP) was formed (Table 2). Moreover, the Prins reaction of (-)-isopulegol with benzaldehyde on K10 and CLOI, functionalized with the same reagent, exhibited a very high selectivity (up to 95%) to chromenols **4** [38].

It is important to note that although halloysite nanotubes and commercial montmorillonite K10 per se with weak to moderate acidity were active in the Prins condensation [40], the efficient catalysis of the Prins-Ritter reaction requires much stronger $-SO_3H$ groups on clay and carbon materials surface (0.33–5.84 mmol H^+ /g, Table 1).

Although acidity of K10-CSA is significantly higher (5.84 mmol H^+ /g) than for other investigated materials (Table 1), the initial rates of

Table 1
Physico-chemical properties of the materials.

Material	S_{BET} , m^2/g	V_{pore} , cm^3/g	d_{pore} , nm	Elemental analysis, mmol/g (wt%)		XPS, mmol/g	Acidity		
				C	S		H^+ , mmol/g	Brønsted, $\mu mol/g$	Lewis, $\mu mol/g$
K10 ^a	247 ^b	0.36 ^b	5.1 ^b	0.07	0	0	0.22	48 ^b	56 ^b
K10-CSA ^a	38	0.162	8.9	0.15	1.42	1.81	5.84	294	0
K10-CSP ^a	155	0.245	3.7	9.73	1.21	0.50	0.8	102	78
CLOI ^a	720 ^c	–	–	0.15	0	0	0.03	–	–
CLOI-CSA ^a	13	0.03	3.6	0.15	1.05	0.90	1.78	140	66
CLOI-CSP ^a	5	0.05	3.6	10.06	1.31	0.59	0.88	161	45
HNT ^a	60 ^b	0.22 ^b	15.7 ^b	0.04	0	0	0.05	13 ^b	21 ^b
HNT-CSA ^a	7	0.06	3.6	0.15	0.84	1.15	2.23	71	15
HNT-CSP ^a	10	0.08	12.0	6.48	0.83	1.25	0.82	27	5
ox-CNT ^d	249	0.62	–	(80.4)	(0)	0	0.05	–	–
CNT-CSP ^d	181	0.47	–	(70.3)	(0.45)	0.15	0.4	–	–
BioC ^e	562	0.305	–	(80.4)	(0)	–	0	–	–
BioC-CSA ^e	129	0.09	–	(69.4)	(1.78)	–	0.332	–	–
BioC-CSP ^e	113	0.06	–	(59.0)	(4.95)	–	0.983	–	–
BioC- H_2SO_4	559	0.29	–	(77.1)	(0.86)	–	0.178	–	–

The data from: ^a[38]; ^b[40]; ^c[52]; ^d[37] and ^e[47]

Measured by ^fpotentiometric titration, and by ^gFTIR with pyridine as a probe molecule

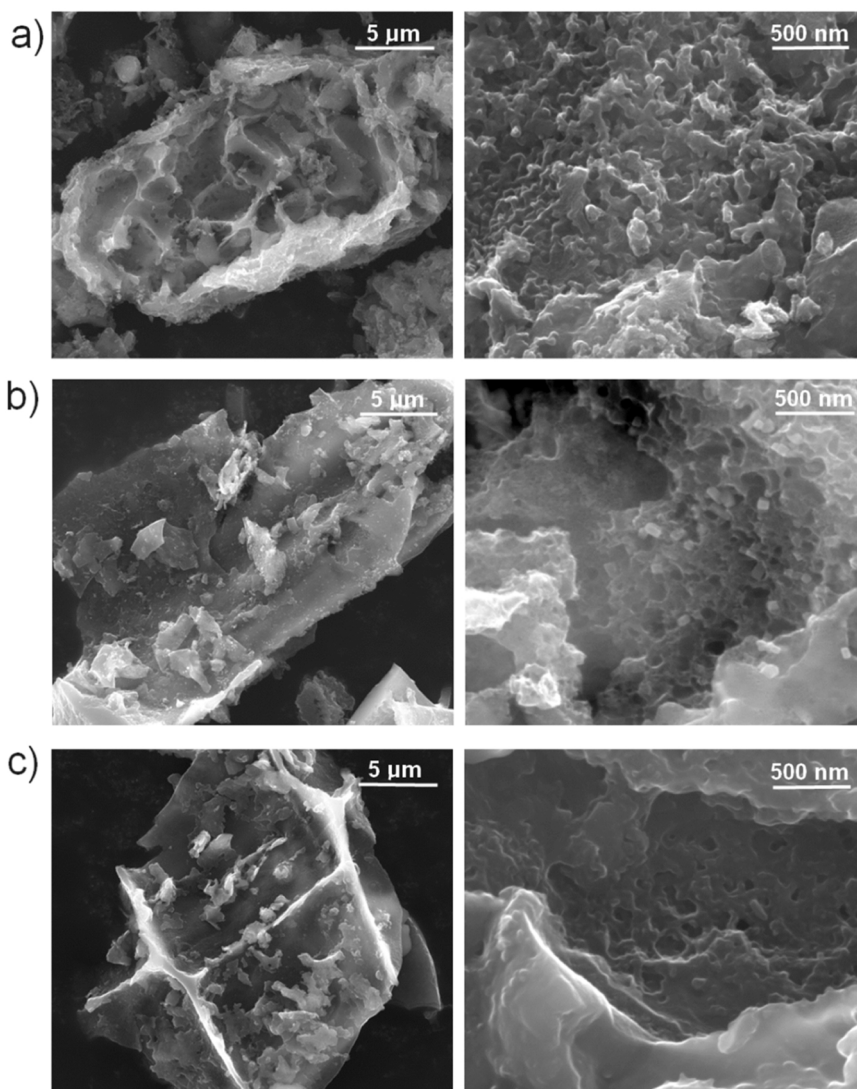


Fig. 3. SEM images of the BioC parent (a) and modified by CSA (b) and CSP (c).

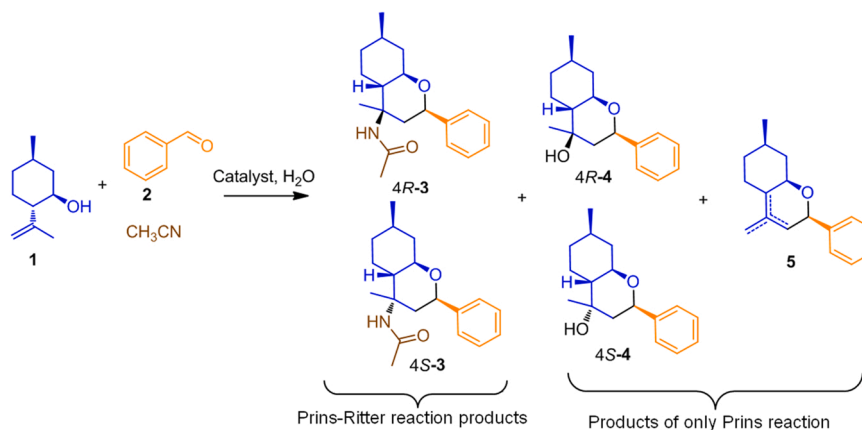


Fig. 4. Products of (-)-isopulegol reaction with benzaldehyde and acetonitrile over investigated catalysts.

(-)-isopulegol consumption (r_0) for this sample and some other catalysts (BioC-CSA/CSP, CNT-CSP) were comparable (Table 2). Moreover, a similar value of the initial reaction rate r_0 was observed for a highly acidic commercial resin Amberlyst-15 bearing total capacity exceeding 1.7 mol/L (Table 2, entry 12). Thus, no apparent dependence for the

Prins-Ritter initial reaction rate on acidity could be seen. The kinetic curves for (-)-isopulegol conversion are shown in Fig. 5.

On the other hand, the largest rate for (-)-isopulegol condensation with benzaldehyde was observed over K10-CSA exhibiting the highest acidity [38]. Complete conversion of this monoterpene also occurred

Table 2

Initial rates for (-)-isopulegol consumption and selectivity at 50% (-)-isopulegol conversion over studied heterogeneous catalysts.

Entry	Catalyst	r_0 mmol/g·min	Time	Selectivity, %						
				Amides 3				Chromenols 4		Dehydration products 5
				Total	4R-3	4S-3	4R/4S	Total	4R/4S	
1	K10-CSA	0.12	60	76.2 ^f	51.2	25.0	2.0	18.8	3.9	4.6
2	K10-CSP	0.05	120	73.5	47.5	26.0	1.8	22.6	3.9	3.7
3	CLOI-CSA	0.04	240	81.8	57.7	24.1	2.4	15.8	3.6	2.1
4 ^b	CLOI-CSP	–	240	68.3	40.7	27.5	1.5	25.6	3.9	5.1
5 ^c	HNT-CSA	–	240	74.2	41.5	32.7	1.3	22.7	4.0	2.4
6	HNT-CSP	0.03	120	56.8	40.7	16.1	2.5	30.8	3.5	12.2
7	BioC-CSA	0.12	60	83.8	71.3	12.5	5.7	13.3	2.5	2.7
8	BioC-CSP	0.10	60	67.4	47.6	19.8	2.4	24.3	3.8	8.0
9 ^d	BioC-H ₂ SO ₄	–	240	78.4	60.7	17.7	3.4	15.3	4.3	3.1
10	CNT-CSP	0.11	60	68.7	53.4	15.3	3.5	21.5	3.4	9.5
11 ^e	CNT-CSA	0.09	60	82.7	69.1	13.6	5.1	15.2	3.4	2.1
12 ^e	Amberlyst-15	0.11	60	47.4	34.8	12.6	2.8	35.0	4.1	16.7

Reaction conditions: 0.65 mmol of (-)-isopulegol, 3.0 mmol of benzaldehyde, 0.1 g of dry catalyst, 17.3 mmol of added H₂O, anhydrous acetonitrile was used both as a reactant and solvent, total volume of the reaction mixture 20 mL, temperature 30 °C.

^aThe initial reaction rates are calculated as changes in the initial concentration of isopulegol at time zero and after 15 min (mmol/L), divided by the reaction time (15 min) and catalyst mass (g).

Achieved conversion for 240 min:

^b18.3%; ^c15.4%; and ^d9%

^eData from [37]

^fValues of selectivity reported with the decimal precision are average values of at least 2–3 experiments

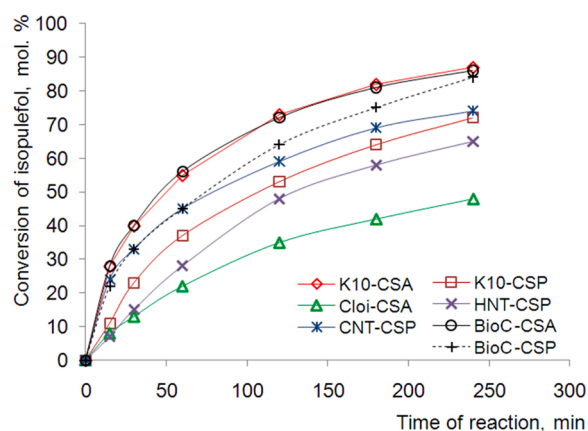


Fig. 5. Conversion of (-)-isopulegol as a function of the reaction time on SO₃H-functionalized catalysts.

on CLOI-CSP and HNT-CSA that were practically inactive in the current study (Table 2, entry 4, 5). Interestingly, for the Prins cyclization of isoprenol with isovaleraldehyde, a clear correlation between r_0 and

acidity of aluminosilicates was found [54].

In summary, the parent clays (montmorillonite, halloysite, cloisite) with a relatively low concentration of Brønsted and Lewis a.s. (up to 100 $\mu\text{mol/g}$, Table 1) are not active in the Prins-Ritter reaction. Subsequently materials containing more acidic SO₃H-groups are required. High selectivity to the target amides (ca. 76–84%) was demonstrated by CSA-treated catalysts (-SO₃H fragments), while on modified by CSP solids (-PhSO₃H moieties), a relatively large amount of the Prins reaction byproducts (up to 43.0%) was formed. The largest selectivity to 4-amido-octahydro-2H-chromenes **3** (ca. 84%) was observed when using a non-acidic starting material, biochar, modified with chlorosulfonic acid which provided acidity of 0.33 mmol H⁺/g.

Over studied catalysts, selectivity to amides **3** somewhat increased with an increase of (-)-isopulegol **1** conversion (Fig. 6a). At the same time, a certain decrease in selectivity towards chromenols **4** was observed (Fig. 6b). This indicates that, under reaction conditions, by-products **4** are partially converted to compounds **3** via first dehydration and a subsequent reaction with acetonitrile (Fig. 7).

It should be noted that the 4R/4S value for the amides also increased with the (-)-isopulegol conversion (Fig. 6a), which may be due to (i) the predominant formation of 4R-**3** during dehydration followed by the interaction with acetonitrile, as well as (ii) dynamic behavior of catalytically active sites. The latter argument is supported by a slight

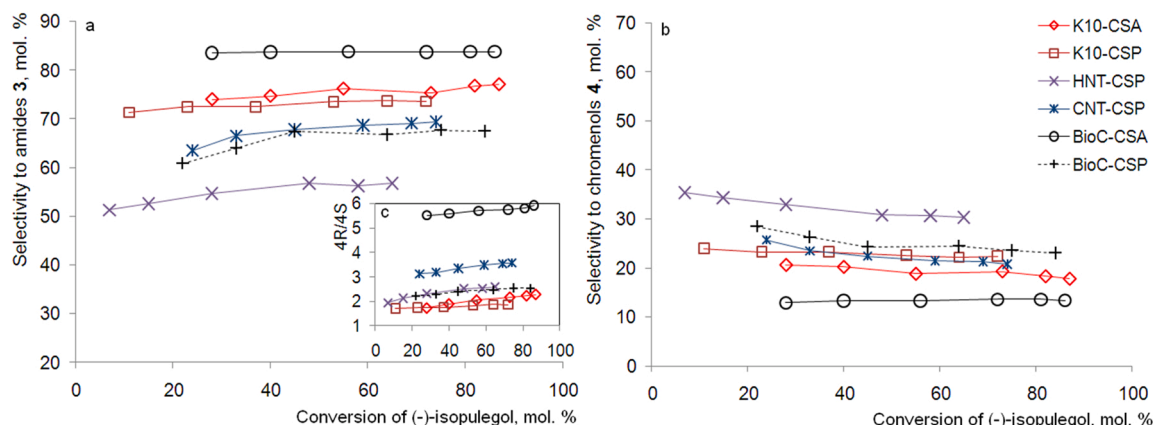


Fig. 6. Selectivity to amides **3** (a), chromenols **4** (b), and 4R-**3**/4S-**3** ratio (c) as a function of (-)-isopulegol conversion on SO₃H-functionalized catalysts.

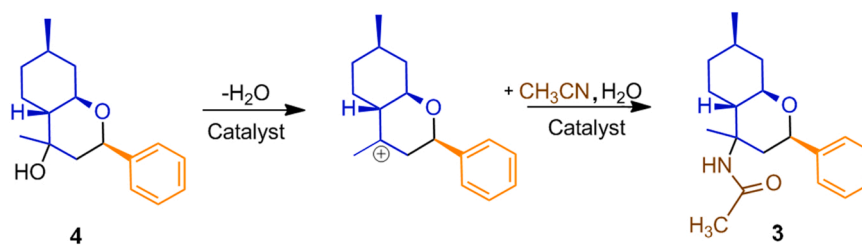


Fig. 7. Scheme for chromenols **4** conversion to amides **3** on SO₃H-functionalized catalysts.

increase in 4R/4S ratio on BioC-CSA (Fig. 6a), whereas selectivity to **3** and **4** was independent on substrate conversion of (Fig. 6).

Selectivity after 240 min is shown in Table S1. A relatively high conversion of (-)-isopulegol (up to ca. 88%) by that time was observed over BioC-CSA/CSP and K10-CSA (Table S2, Fig. 5).

Thus, from the kinetic viewpoint the Prins-Ritter reactions proceeds in a parallel way with a slight contribution of the consecutive path apparent from a minor selectivity increase to amides **3** with (-)-isopulegol conversion due to a partial conversion of compounds **4** to **3**.

3.2.2. Influence of the reaction conditions

The effect of temperature and reagent concentration was studied in the presence of BioC-CSA, since it displayed high activity and the largest selectivity in the Prins-Ritter reaction.

With an increase in the reaction temperature, there was some decrease in selectivity to the amides **3** and an increase in selectivity to the Prins condensation products **4** and **5** at the same conversion level (Table 3). In the case of chromenols, no significant changes in the 4R/4S ratio were observed when changed temperature. At the same time, a significant increase in the diastereomers ratio for compounds **3** also occurred when decreased temperature from 40 °C to 20 °C. This change in stereoselectivity indicates the kinetic control for the formation of the 4R-isomer of amide **3** and is consistent with the results obtained previously in [37].

Thus, the total yield of products **3** and the 4R/4S stereoisomers ratio can be slightly increased by lowering the reaction temperature at the expense of lower reaction rates. Nevertheless, even at 30 °C, selectivity to amides **3** over BioC-CSA (ca. 84%, Table 3) was significantly higher than their yield at -25 °C in the presence of a homogeneous catalyst – triflic acid (62%) [8].

A set of experiments were performed at different initial concentrations of the reagents, which varied by the total volume of the reaction mixture. The amounts of (-)-isopulegol, benzaldehyde and water were the same, while the amount of acetonitrile was changing.

With a decrease in the initial concentration of (-)-isopulegol (and, respectively, water) in the reaction mixture, there was a significant increase in selectivity to amides **3** and its decrease to products **4** and **5** (Table 4). Because even at the highest initial concentration of (-)-isopulegol there is a significant excess of acetonitrile (ca. 150:1), these results should be related to the influence of water as discussed in more detail below.

In addition to changes in selectivity depending on the dilution with acetonitrile, a decrease in the 4R/4S ratio for compounds **3** was also observed. The highest yield of 4R-**3** (ca. 71%, Table 4) was achieved at the initial (-)-isopulegol concentration of 0.032 mol/L, and no further increase in the total amides yield was observed in more dilute solutions (Table 4).

A decrease in the overall selectivity to amides **3** with increasing water concentration may be due to an increase in the hydration rate, and, accordingly, selectivity to chromenols **4**, as well as 4R-**4**/4S-**4** ratio value (Table 4, Fig. S3). Indeed, according to [40] in the condensation of monoterpenoid **1** with thiophene-2-carbaldehyde, an increase of H₂O amount on the catalyst surface led to a sharp increase in both yield and stereoselectivity with respect to chromenols.

On the other hand, an increase in the water concentration in the reaction mixture also led to an increase in the stereoselectivity towards amides **3**, i.e. predominance of a kinetically controlled compound 4R-**3**, which is consistent with the results obtained in [37]. A detailed discussion of the reaction mechanism is given below.

3.2.3. Analysis of sulfonic groups leaching (filtration tests)

It is well-known that in some cases for the reactions over catalysts bearing SO₃H-groups, the sulfonic group can be leached away from the catalyst surfaces [45,46]. Therefore, with the aim to evaluate leaching of such groups in the current case, the catalyst was removed after 30 min from the reaction mixture and the remaining solution was left under constant stirring at the same reaction conditions.

The results indicate that in the case of BioC-CSP and CNT-CSP, no further reaction was observed after their separation from the mixture, while K10-CSP exhibited some increase in the conversion of (-)-isopulegol (Fig. 8). In the case of K10-CSA and BioC-CSA, the reaction continued after the catalyst removal pointing out on leaching of sulfonic groups. Moreover, in the experiment with BioC-CSA, the conversion after 180 min was 83% being practically the same as without filtration (Fig. 8). Note that selectivity after 180 min for the samples that were leached (K10-CSA, BioC-CSA, K10-CSP) was comparable to the results when there was no filtration (Table S2).

It should be noted that carbon materials subjected to carbonization at a temperature > 700 °C before sulfonation (as in the case of BioC) can be deactivated due to leaching, since C(sp³)-SO₃H bonds in the absence of electron-withdrawing groups are weakly stable [45]. Thus, under the Prins-Ritter reaction conditions, when water is present, SO₃H-groups are

Table 3

Selectivity at 50% (-)-isopulegol conversion and different reaction temperatures on BioC-CSA catalyst.

Entry	Temperature, °C	Time, min	Selectivity ^a , %						
			Amides 3				Chromenols 4		Dehydration products 5
			Total	4R- 3	4S- 3	4R/4S	Total	4R/4S	
1	20	120	84.1	74.0	10.1	7.3	12.5	2.8	3.0
2	30	60	83.8	71.3	12.5	5.7	13.3	2.5	2.7
3	40	15	79.3	64.6	14.7	4.4	16.7	2.2	3.7

Reaction conditions: 0.65 mmol of (-)-isopulegol, 3.0 mmol of benzaldehyde, 0.1 g of dry catalyst, 17.3 mmol of added H₂O, anhydrous acetonitrile was used both as a reactant and a solvent, total volume of the reaction mixture 20 mL, temperature 30 °C.

^aValues of selectivity reported with the decimal precision are average values of at least 2–3 experiments

Table 4

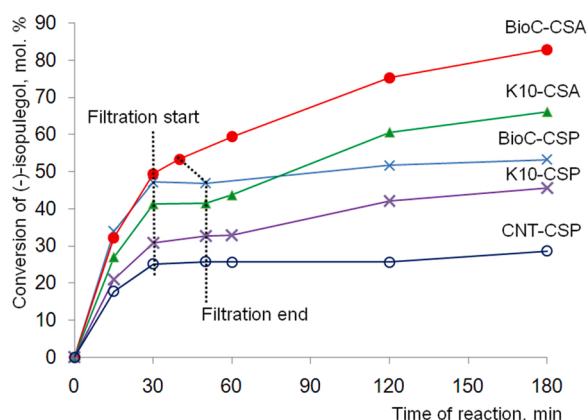
Selectivity at 50% (-)-isopulegol conversion and different initial concentrations of the reagents over BioC-CSA catalyst.

Entry	Initial concentration ^a , mol/L		Time, min	Selectivity, %						
	(-)-Isopulegol	Water		Amides 3				Chromenols 4		Dehydration products 5
				Total	4 <i>R</i> - 3	4 <i>S</i> - 3	4 <i>R</i> /4 <i>S</i>	Total	4 <i>R</i> /4 <i>S</i>	
1	0.13	3.46	30	62.3 ^b	54.2	8.1	6.7	30.3	3.5	6.2
2	0.065	1.73	60	72.9	63.3	9.6	6.6	22.7	3.2	4.0
3	0.032	0.87	60	83.8	71.3	12.5	5.7	13.3	2.5	2.7
4	0.022	0.58	60	83.4	69.4	14.0	5.0	12.0	2.0	3.6
5	0.013	0.35	120	83.6	67.3	16.3	4.1	10.6	1.3	4.6

Reaction conditions: 0.65 mmol (-)-isopulegol, 3.0 mmol benzaldehyde, 0.1 g of dry catalyst, anhydrous acetonitrile both as a reactant and a solvent, 17.3 mmol (0.311 g) of added water, temperature 30 °C.

^aInitial concentration of the reagents was reduced by increasing of the total volume of the reaction mixture

^bValues of selectivity reported with the decimal precision are average values of at least 2–3 experiments

**Fig. 8.** Conversion of (-)-isopulegol as function of reaction time in the tests with catalyst filtration.

washed away when using CSA-functionalized catalysts. This is clearly confirmed by (i) a significant decrease in the catalyst acidity after filtration (Table S2, entry 2) and (ii) value of filtrate pH < 2 (test with indicator paper).

On the other hand, sulfonic groups in BioC-CSP and CNT-CSP were not leached (Fig. 8), which indicates stability of C-O-Si bonds during the reaction. In addition, for K10-CSP, which exhibited less leaching, a relatively minor decrease of acidity was observed (Table S2, entry 4). On the other hand, in the Prins reaction of isopulegol with benzaldehyde on K10-CSP in the absence of water, leaching was not observed [38]. This

clearly indicates that washing away of the active groups from this catalyst in the Prins-Ritter reaction occurs due to the presence of water.

Thus, although the leaching-resistant catalyst BioC-CSP exhibited moderate selectivity to amides 3 (ca. 67%, Table 2) at 30 °C, it was higher than over commercial Amberlyst-15 (ca. 47%) under the same conditions, as well as in the presence of TfOH at – 25 °C (62% [8]). Apparently, the future work should concentrate on synthesis of most robust heterogeneous catalysts affording excellent selectivity to the Prins-Ritter reaction products.

3.2.4. Homogeneous catalysis

In the case of homogeneous catalysis investigated in this work, the main products of (-)-isopulegol condensation with benzaldehyde in acetonitrile were amides 3 (Table 5). When the reaction was performed without water, a high overall selectivity to these products (ca. 80%) was achieved with sulfuric acid and oleum (Table 5, entry 1 and 4), while with chlorosulfonic and *p*-toluenesulfonic (*p*-TSA) acids significant amounts of dehydration products were observed (up to ca. 37, Table 5, entry 6 and 9).

Addition of water before the reaction not only increases the overall yield of amides 3, but also leads to the stereoselectivity inversion. Namely without water, the reaction mixture was dominated by 4S-3, while after addition of 17.3 mmol of H₂O, 4R-isomer of 3 was the main product in all cases (Table 5). At the same time, an increase in selectivity to chromenols 4 and a decrease in selectivity to the dehydration products 5 were also observed. The highest yield of amides 3 after adding water was for sulfuric acid (ca. 82%) with the 4R/4S value of 6.3 (Table 5, entry 3).

An interesting fact is that with H₂SO₄ and oleum without any water

Table 5

(-)-Isopulegol conversion and selectivity after 180 min for investigated homogeneous and heterogeneous catalytic reactions.

Entry	Catalyst	Added H ₂ O, mmol	Conversion, %	Selectivity, %						
				Amides 3				Chromenols 4		Dehydration products 5
				Total	4R-3	4S-3	4R/4S	Total	4R/4S	
1	H ₂ SO ₄	0	84	80.6 ^b	32.1	48.5	1:1.5	7.6	1:1.7	11.3
2		2.2	100	81.9	58.0	23.9	2.4:1	11.1	1:1.3	6.8
3		17.3	100	81.4	70.3	11.1	6.3:1	15.2	1.7:1	3.1
4	Oleum, 20% SO ₃	0	94	76.0	25.2	50.8	1:2.0	7.7	1:1.7	14.6
5		17.3	100	81.8	69.2	12.6	5.5:1	15.8	1.9:1	2.2
6	HSO ₃ Cl	0	90	61.4	14.4	47.0	1:3.3	4.8	3.8:1	33.5
7		17.3	100	80.9	65.6	15.3	4.3:1	12.3	2.6:1	3.5
8	BioC-CSA	17.3	81	83.8	71.5	12.3	5.8:1	13.6	2.3:1	2.6
9	<i>p</i> -TSA	0	100	44.8	7.5	37.3	1:5.0	17.7	2.8:1	37.3
10 ^a		2.2	100	64.1	14.9	49.2	1:3.3	17.9	4.1:1	18.0
11 ^a		17.3	100	70.3	50.6	19.7	2.6:1	20.6	3.9:1	9.1
12	BioC-CSP	17.3	75	67.7	48.6	19.1	2.5:1	23.6	3.6:1	8.3

Reaction conditions: 0.65 mmol of (-)-isopulegol, 1.95 mmol of benzaldehyde, 0.65 mmol of a liquid catalyst or 0.1 g of a solid one, anhydrous acetonitrile was used both as a reactant and a solvent, the total volume of the reaction mixture 20 mL, temperature 30 °C

^aThe data from [37]

^bValues of selectivity reported with the decimal precision are average values of at least 2–3 experiments

addition, the 4*S*-isomer of chromenol **4** was predominantly formed (Table 5, entry 1 and 4), while in all other cases 4*R*-**4** was observed. Moreover, 4*R*-chromenol was also the main product in the conventional Prins reaction [38,40].

It is important to note that with either sulfuric and chlorosulfonic acids or BioC-CSA, selectivity to the Prins-Ritter reaction products **3** and the 4*R*/4*S* ratio were similar (Table 5). This can be explained by the fact that H₂SO₄, which is an efficient catalyst for the amides **3** formation, is formed under the reaction conditions from HSO₃Cl by hydrolysis or from leaching of unstable BioC-CSA.

On the other hand, selectivity to **3** with *p*-TSA and over leaching-resistant BioC-CSP was also similar (ca. 70%, Table 5), wherein these catalysts have identical -PhSO₃H moieties (Fig. 2). Therefore, such active sites work with the same selectivity in the case of both homogeneous and heterogeneous catalysis. Based on this, it can be assumed that stable to deactivation carbon catalysts with directly fixed functional groups (C-SO₃H) should also provide high overall and stereo selectivity to amides.

3.2.5. Mechanistic considerations

The mechanism of the Prins-Ritter reaction is discussed here on the basis of both experimental work and detailed DFT calculations for all products and intermediates expanding substantially the previous work [37] where only relative energies for amides were considered. The simulations were performed using sulfuric and *p*-toluenesulfonic acids as models of catalysts containing -SO₃H (CSA) and -PhSO₃H (CSP) groups, respectively.

The proposed mechanism for the reaction is shown in Fig. 9. Initially, (-)-isopulegol **1** reacts with the protonated form of benzaldehyde **2** which leads to a non-cyclic adduct. Because of the *exo* C=C bond of

(-)-isopulegol and the electrophilic character of the carbon, further cyclization occurs with the formation of intermediate **3-A**, which then undergoes multiple transformations. Thus, the addition of acetonitrile to **3-A** gives intermediates **3-B** and **3-C**, which are precursors of 4*R*- and 4*S*-amide, respectively. Alternatively, the cation **3-A** can undergo either direct hydration to form chromenols **4**, or deprotonation leading to products **5**.

According to the DFT calculations, in the case of H₂SO₄ as a catalyst, the relative energy of the intermediate **3-A** is 49.8 kJ/mol (Fig. 10). After acetonitrile addition to this intermediate, the energy for the resulting **3-C** cation increases to 55.2 kJ/mol, which is 13.8 kJ/mol higher than for **3-B**. The further formation of 4*S*-amide from **3-C** is thermodynamically the most favorable (-31.4 kJ/mol) among all reaction products, being 32.3 kJ/mol lower than for 4*R*-**3** (Fig. 10). Optimized structures of intermediates and products are shown in Table S3.

Indeed, with homogeneous catalysts H₂SO₄, oleum and HSO₃Cl at 30 °C without adding water, the main product was 4*S*-amide (ca. 47–51%, Table 5), which, according to the DFT predictions, should be formed as a result of thermodynamic control of the reaction. Under the same conditions 4*S*-isomer of **3** also was predominant (up to ca. 34%) among amides over K10-CSA and CNT-CSA [37]. On the other hand, conducting the experiments at 0 °C on K10-CSA [37], or -25 °C in the presence of TfOH [8] led mainly to 4*R*-amides, which clearly indicates the kinetic control of the reaction. In the same way, the selectivity to 4*R*-isomer on BioC-CSA increased with a decrease in the reaction temperature (Table 3). It should be noted that the energy difference for amides **3** calculated in this work (32.3 kJ/mol) is in a better agreement with the experimental results than that previously obtained (1.1 kJ/mol) in [37].

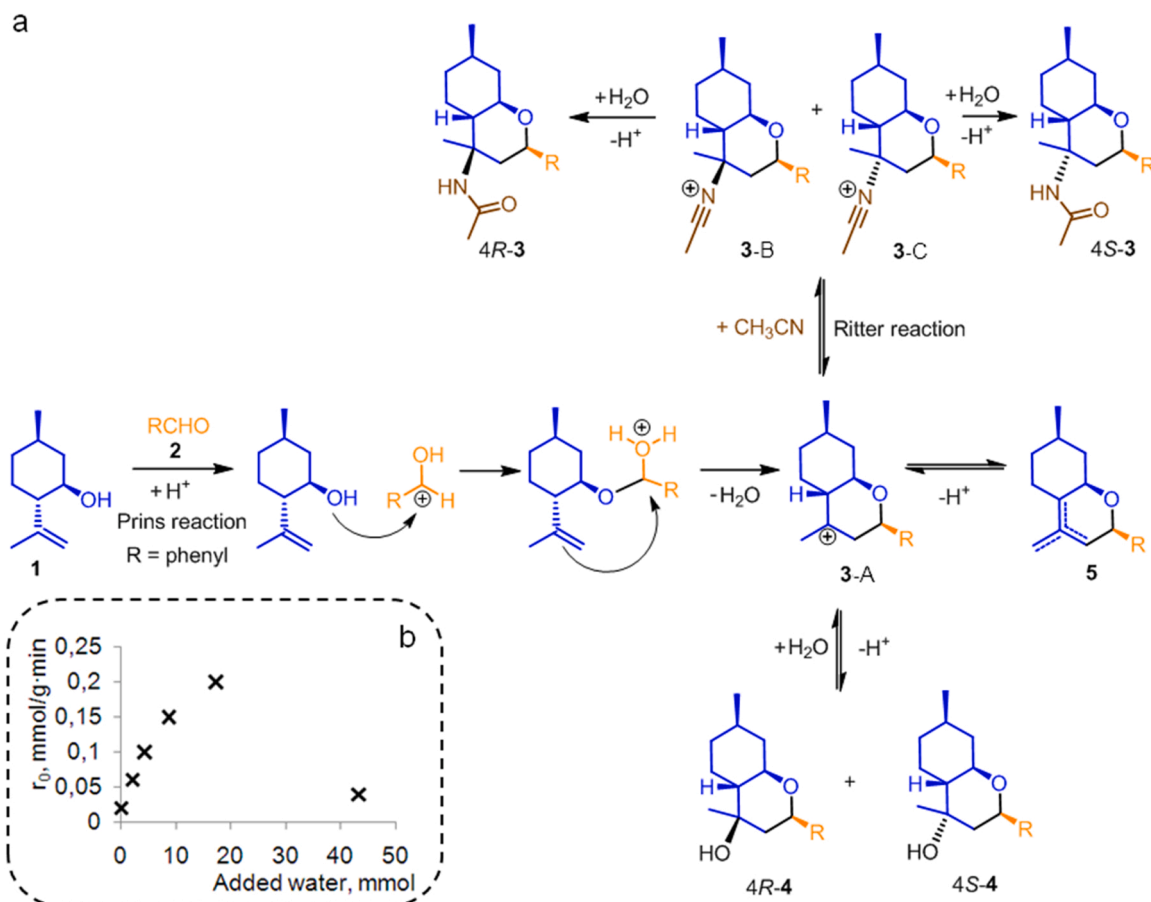


Fig. 9. Mechanism of the Prins-Ritter reaction (a), and the initial rate of (-)-isopulegol consumption depending on water added on K10-CSA (b, data from [37]).

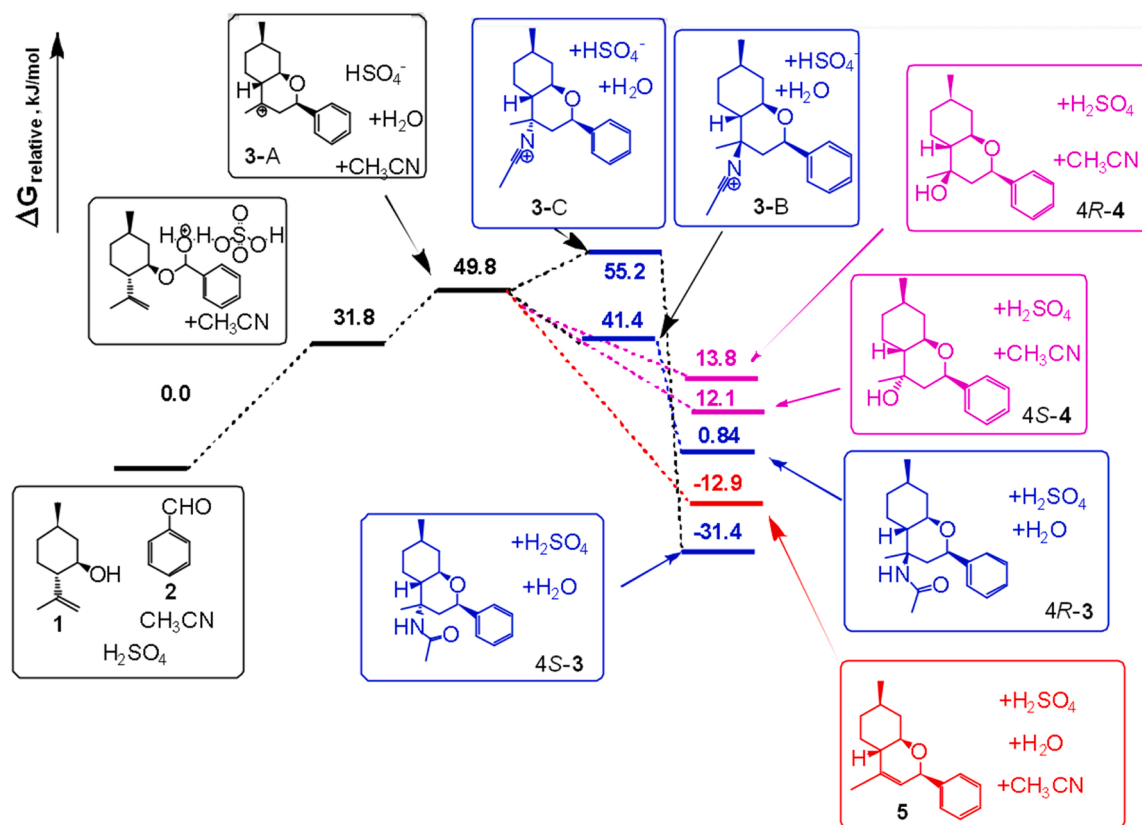


Fig. 10. DFT calculated energy diagram for the Prins-Ritter reaction on sulfuric acid as a catalyst.

Formation of the dehydration products **5** due to deprotonation of the intermediate **3-A** is also thermodynamically favorable (-12.9 kJ/mol). Thus, in the case of using sulfuric acid and oleum without water, selectivity to compounds **5** was up to ca. 15% (Table 5) exceeding that for chromenols **4**. An even higher yield of products **5** was observed in the presence of HSO_3Cl (33.5%), as well as with K10-CSA and CNT-CSA (up to 43.9% [37]).

Quantum chemical calculations showed that under the Prins-Ritter conditions for the reaction with sulfuric acid, the formation of chromenols **4** is the least beneficial, and **4S-4** is 1.7 kJ/mol more stable than **4R-4** (Fig. 10). Indeed, without water for all homogeneous catalysts studied, alcohols **4** were minor products (Table 5), however, the thermodynamically more stable isomer **4S-4** prevailed only in the case of H_2SO_4 and oleum (Table 5, entry 1 and 4).

On the contrary, in the case of the Prins reaction [38,40,55] as well as the Prins-Ritter reaction (Table 2) on the modified solid catalysts, the **4R**-isomer of chromenol **4** predominated. However, it was shown that under the acid catalysis conditions, dehydration of **4R-4** to compounds **5**, as well as minor isomerization to **4S-4** can occur [55]. Although both processes are energetically favorable (Fig. 10) apparently their rates are low.

Thus, although simulation show that formation of chromenols **4** is thermodynamically unfavorable ($\Delta G > 0$), the general appearance of the diagram (Fig. 10) agrees well with the experimental results, predicting that the **4S**-isomer **3** is the most beneficial product, and chromenols can spontaneously convert to dehydration products **5**.

DFT computations for the Prins-Ritter reaction in the presence of *p*-toluenesulfonic acid (Fig. S4) show that the relative energies for intermediates **3-A** (80.8 kJ/mol) as well as **3-B** (86.6 kJ/mol) and **3-C** (72.6 kJ/mol) become higher than in the case of sulfuric acid, however, the general form of the diagram and the difference between the amide precursors **3-B** and **3-C** (14.0 kJ/mol) practically does not change. The main products with *p*-TSA are also amides **3** with a predominance of the

4S-isomer as a result of the thermodynamic control. In this case, the overall selectivity to compounds **3** (ca. 45%) was significantly lower than for sulfuric acid (81%), while formation of ca. 37% of the dehydration products was observed (Table 5, entry 9). Thus, under the reaction conditions (30 °C), the course of the Prins reaction through deprotonation or hydration of **3-A** ion becomes more pronounced. Note that on catalysts containing $-\text{PhSO}_3\text{H}$ groups (CSP-modified ones), the Prins-Ritter reaction proceeds with lower selectivity to amides (Table 2).

The role of water in the Prins-Ritter reaction requires a detailed discussion. According to the reaction pathway, the step that determines stereoselectivity is the addition of acetonitrile to **3-A** ion, followed by hydration of intermediates **3-B** and **3-C**, resulting in the formation of **4R**- and **4S**-amides, respectively (Fig. 10). Thus, in the case when water was not added, the main product at 30 °C in the presence of homogeneous (Table 5) and heterogeneous (K10-CSA, CNT-CSA [37]) catalysts is the thermodynamically favorable **4S-3**. Subsequently, the concentration of **3-C** species should be significantly higher than **3-B**.

However, addition of H_2O to the system resulted in both a dramatic increase in **4R**-amide selectivity (Table 5, Fig. S1) and the initial rate of (-)-isopulegol consumption r_0 (Fig. 10b), indicating a change to kinetic control of the reaction. It can be assumed that under excess of water, the rate of hydration of **4R**-amide precursor **3-B** is much higher than that for **3-C**. Accordingly, the $\text{3-C} \leftrightarrow \text{3-A} \leftrightarrow \text{3-B}$ equilibrium shifts towards **3-B** formation, and this stereoselectivity responsible step ($\text{3-A} \rightarrow \text{3-B}$) should define the reaction rate. Moreover, the addition of water also led to a sharp decrease in the selectivity for products **5**, accordingly, addition of acetonitrile to **3-A** becomes more preferable than alternative deprotonation.

The highest initial rate of (-)-isopulegol consumption on K10-CSA was observed after the addition of 17.3 mmol H_2O , while an increase in its amount to 43.3 mmol led to a decrease in the r_0 value (Fig. 10b) and some increase in selectivity towards chromenols **4**. This may be due to solvation of (i) catalytically active sites and (ii) adsorbed species [56],

such as 3-A. Similarly, the yield of products 4 on BioC-CSA increased from ca. 11–30% with increasing initial water concentration from 0.35 mol/L to 3.46 mol/L, respectively (Table 4).

Thus, based on the above, DFT calculations and experimental results show that under mild conditions (30 °C) formation of 4S-amide is more beneficial than of alcohols and dehydration products. Nonetheless the yields of amides on heterogeneous catalysts did not exceed 44%. However, the addition of water causes a dramatic increase in the reaction rate and selectivity to 4R-amide due to a change to a kinetic control, resulting in both high amides yields and stereoselectivity (up to 84%, 4R/4S of 5.7).

3.2.6. Kinetic modelling

Kinetic modelling was done based on the mechanistic ideas discussed above (Fig. 6) considering essentially parallel formation of products through the common intermediate.

The simplified reaction network corresponding to this assumption is presented in Fig. 11.

For the reaction network it was assumed that there are transformations between 4S-3 and 4R-3 in line with dependences of 4R/4S ratio with conversion. Because the aldehyde was used in excess, and even so acetonitrile, the reaction order in these compounds was assumed to be equal to zero giving the following kinetic equations:

$$r_1 = k_1 c_{iso}; r_2 = k_2 c_{iso}; r_3 = k_3 c_{iso}; r_4 = k_4 c_{iso} r_5 = k_5 c_{iso}; r_6 = k_6 c_{4S3} \quad (1)$$

Where the constants also include catalyst concentration, and c_{iso} , c_{4S3} are the concentration of (-)-isopulegol and 4S-3 compounds respectively. The mass balances for the components are

$$\begin{aligned} \frac{dc_{iso}}{dt} &= -r_1 - r_2 - r_3 - r_4 - r_5; \frac{dc_{4R4}}{dt} = r_1; \frac{dc_{4S4}}{dt} = r_2; \frac{dc_{4S3}}{dt} \\ &= r_5 - r_6; \frac{dc_{4R3}}{dt} = r_4 + r_6; \frac{dc_5}{dt} = r_3 \end{aligned} \quad (2)$$

The backward difference method was used to solve a system of ordinary differential Eq. (2) a subtask to the parameter estimation with the Levenberg-Marquardt and/or Simplex method using software ModEst [57].

In the preliminary calculations it became apparently clear that the model represented by Eqs. (1) and (2) requires some modifications, as concentration profiles exhibited deviations from the first order dependences. Previously [37] the authors addressed the influence of water in the Prins condensation for synthesis of octahydro-2H-chromen-4-ols, concluding that water stored in halloysite nanotubes is involved in these reactions. A detailed mechanism of the water influence from a kinetic point of view apparently requires a dedicated study, thus as the first approach a conversion (x) dependent activity function a was introduced for transformations of (-)-isopulegol:

$$\frac{dc_{iso}}{dt} = a(-r_1 - r_2 - r_3 - r_4 - r_5) = (1 - k_a x)(-r_1 - r_2 - r_3 - r_4 - r_5) \quad (3)$$

where the constant k_a reflects in general the influence of water on the catalyst. Other approaches often applied in catalytic reaction engineering to account for activity changes during catalysis have been also tested including an exponential decay as a function of either conversion

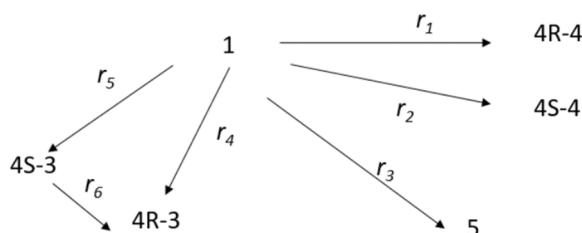


Fig. 11. Simplified reaction network.

or time [58]. Rather similar results from the mathematical viewpoint have been obtained, thus the treatment here is limited only to Eq. (3).

The estimated parameters are listed in Table 6 and the comparison between experimental data (points) and calculated concentration curves is shown in Fig. S6 confirming that the model can describe the experimental data. The degree of explanation was typically above 99%.

The kinetic constants for the primary reactions (1–5 in Fig. S5) are in general well identified with rather low values of errors. Large errors for k_6 are related to the structure of the kinetic model, as this constant represents consecutive transformations of the primary product which are not profound. Subsequently the constant of such transformations of the primary product is statistically less reliable. The values of k_a reflecting the influence of water indicate that the influence of water is more prominent for HNT-CSP catalyst.

3.2.7. Reaction scope

The Prins-Ritter reaction of (-)-isopulegol with various aldehydes in acetonitrile has been studied with sulfuric acid as a homogeneous catalyst, since it showed high both total and stereoselectivity to amides 3, comparable to BioC-CSA, which is not resistant to leaching.

In the presence of 1 eq of H_2SO_4 and 17.3 mmol of water at 30 °C after 180 min complete conversion of (-)-isopulegol 1 was observed in all cases (Table 7). For studied aldehydes, a high (up to ca. 85%) selectivity to octahydro-2H-chromene amides 3 with a 4R/4S ratio of up to 7.5 was observed (Table 7). At the same time, selectivity to 4R-3 was relatively high both in the case of electron-donating and electron-accepting substituents in the aromatic ring, although predominant formation of 4S-chromenol 4 was observed for 4-nitrobenzaldehyde (Table 7, entry 4).

It is worth noting that with TfOH at – 25 °C, both the yields and the ratio of stereoisomers for the resulting amides were lower than in the present work. For example, in the case of thiophene-2-carbaldehyde, it was 64% (4R/4S of 3.5) [8], while with H_2SO_4 selectivity was ca. 85% with the stereoisomers ratio of 5.2 (Table 7, entry 5). Thus, the use of a simple homogeneous catalyst such as H_2SO_4 in combination with water addition makes it possible to achieve high selectivity values for the desired amides under mild conditions.

4. Conclusion

The Prins-Ritter cascade reaction was studied to prepare (-)-isopulegol-derived 4-amidotetrahydropyran compounds (as 4R- and 4S-isomers) under ambient conditions with a number of SO_3H -containing heterogeneous (biochar, carbon and halloysite nanotubes, montmorillonites) and homogenous (H_2SO_4 , HSO_3Cl , p -TSA) catalysts. The solids were functionalized with chlorosulfonic acid (CSA), 2-(4-chlorosulfonylphenyl)ethyltrimethoxysilane (CSP) and H_2SO_4 , giving materials previously thoroughly characterized by a range advanced physicochemical methods.

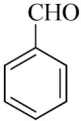
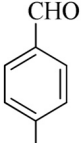
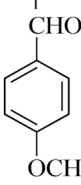
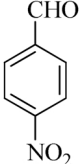
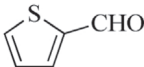
The Prins condensation proceeds efficiently on weak acid sites, whereas the Prins-Ritter cascade requires sulfated materials with strong (0.33 – 5.8 mmol/g) Brønsted acidity. The largest yield of 4-amido-octahydro-2H-chromene (84%) and the 4R/4S isomers ratio (5.7) was observed on biochar, modified with chlorosulfonic acid (BioC-CSA), while on modified by CSP solids a relatively large amount of the Prins reaction byproducts (up to 43%) was formed. Selectivity to the target products and its 4R/4S ratio on BioC-CSA also increased with decreasing temperature or the initial reagent concentration. The carbon materials functionalized by CSP were stable, while catalysts modified with chlorosulfonic acid deactivated by leaching $-SO_3H$ groups. Although the leaching-resistant Biochar-CSP exhibited moderate selectivity to amides (67%) at 30 °C, it was higher than that on the commercial catalyst Amberlyst-15 (ca. 47%). Similar selectivity to the target products on Biochar-CSA ($-SO_3H$ moieties) and H_2SO_4 (81–84%) as well as on Biochar-CSP ($-PhSO_3H$) and with p -toluenesulfonic acid (67–70%) was observed.

Table 6Estimated kinetic parameters and their errors, units of constants in min⁻¹, errors in %.

Param.	BioC-CSA		BioC-CSP		CNT-CSP		HNT-CSP		K10-CSA		K10-CSP	
	Value	Error	Value	Error	Value	Error	Value	Error	Value	Error	Value	Error
k ₁	8.9 10 ⁻⁴	15.2	1.2 10 ⁻³	5.1	0.81 10 ⁻³	13.0	1.2 10 ⁻³	5.6	1.3 10 ⁻³	8.9	1.1 10 ⁻³	10.7
k ₂	4.8 10 ⁻⁴	27.8	3.8 10 ⁻⁴	16.3	2.8 10 ⁻⁴	41.4	3.8 10 ⁻⁴	16.6	3.6 10 ⁻⁴	30.3	2.7 10 ⁻⁴	38.7
k ₃	2.8 10 ⁻⁴	48.2	6.0 10 ⁻⁴	10.4	5.17 10 ⁻⁴	20.2	6.6 10 ⁻⁴	9.8	4.6 10 ⁻⁴	23.4	2.2 10 ⁻⁴	46.9
k ₄	6.3 10 ⁻³	5.9	3.7 10 ⁻³	4.7	3.2 10 ⁻³	10.6	2.0 10 ⁻³	8.6	5.1 10 ⁻³	5.9	2.7 10 ⁻³	9.3
k ₅	1.1 10 ⁻³	32.4	1.4 10 ⁻³	12.0	0.85 10 ⁻³	39.1	0.8 10 ⁻³	21.7	2.0 10 ⁻³	14.9	1.5 10 ⁻³	19.9
k ₆	2.2 10 ⁻⁷	> 200	0.5 10 ⁻⁶	> 200	0.3 10 ⁻⁷	> 200	0.5 10 ⁻⁵	> 200	3.9 10 ⁻⁷	> 200	0.4 10 ⁻⁵	> 200
k _a	0.087	102	0.054	101	0.4 10 ⁻⁵	> 200	0.17	56.1	> 200	> 200	0.8 10 ⁻⁵	> 200
DE*	99.44		99.74		99.19		99.67		99.44		99.12	

* Degree of explanation

Table 7Selectivity in the Prins-Ritter reaction of (-)-isopulegol with a number of aldehydes in acetonitrile for 180 min with H₂SO₄ as a catalyst^a.

Entry	Aldehyde	Conversion after 3 h, %	Selectivity ^b , %						
			Amides 3				Chromenols 4		Dehydration products 5
			Total	4R-3	4S-3	4R/4S	Total	4R/4S	
1		100	81.4	70.3	11.1	6.3	15.2	1.7:1	3.1
2			75.9	65.4	10.5	6.2	16.7	3.1:1	1.5
3			83.3	72.6	10.7	6.8	13.7	5.1:1	2.1
4			73.2	64.6	8.6	7.5	21.2	1:2.2	4.9
5			85.2	71.9	13.3	5.2	12.8	2.1	1.6

Reaction conditions: 0.65 mmol of (-)-isopulegol, 1.95 mmol of aldehyde, 0.65 mmol of catalyst, anhydrous acetonitrile was used both as a reactant and solvent, the total volume of the reaction mixture 20 mL, temperature 30 °C.

^aWith 17.3 mmol of added water^bValues of selectivity reported with the decimal precision are average values of at least 2–3 experiments

DFT calculations and the experimental results show that at 30 °C without adding water formation of 4S-amide is more beneficial than alcohols and dehydration products. However, H₂O addition causes a dramatic increase in the reaction rate and selectivity to 4R-amide due to a change to the kinetic control, resulting in both high amides yields and stereoselectivity. The proposed reaction pathways have been also confirmed by kinetic modeling taking into account the effect of water on the catalyst. Further work should include development of stable heterogeneous catalysts with excellent selectivity towards the Prins-Ritter reaction products.

CRedit authorship contribution statement

A.Yu. Sidorenko Writing – Original draft, conceptualization, Yu.M.

Kurban Investigation. A.F. Peixoto Investigation. N.S. Li-Zhulanov Investigation. J.E. Sánchez-Velandia Investigation. A. Aho Investigation. J. Wärnå Formal analysis. Y. Gu Investigation. K.P. Volcho Supervision. N.F. Salakhutdinov Project administration. D.Yu. Murzin Supervision, Writing - Review & Editing. V.E. Agabekov Funding acquisition.

Declaration of Competing Interest

The authors declare that they have no known competing financial interests or personal relationships that could have appeared to influence the work reported in this paper.

Data Availability

Data will be made available on request.

Acknowledgments

This work is part of the scientific activity of the Institute of Chemistry of New Materials, funded by the National Academy of Sciences of Belarus. Julián E. Sánchez thanks to Pontificia Universidad Javeriana for providing computational powder and to Universidad Jaume I (Pla de Promoció de la Investigació de la Universitat Jaume I) for the Post Doctoral Fellowship. Part of this work (synthesis and characterization of sulfonic-acid catalysts presented in Fig. 2) was funded by the Portuguese funds through Fundação para a Ciência e a Tecnologia (FCT/MCTES) in the framework of the projects UIDB/50006/2020, UIDP/50006/2020. A.F.P. is also grateful to FCT for funding through the Individual Call to Scientific Employment Stimulus 2020.01614.CEECIND/CP1596/CT0007.

Appendix A. Supporting information

Supplementary data associated with this article can be found in the online version at [doi:10.1016/j.apcata.2022.118967](https://doi.org/10.1016/j.apcata.2022.118967).

References

- [1] V. Froidevaux, C. Negrell, S. Cailloil, J.P. Pascault, B. Boutevin, *Chem. Rev.* 116 (2016) 14181–14224.
- [2] M.E. Chen, X.W. Chen, Y.H. Hu, R. Ye, J.W. Lv, B. Li, F.M. Zhang, *Org. Chem. Front.* 8 (2021) 4623–4664.
- [3] D.G. Brown, J. Boström, *J. Med. Chem.* 59 (2016) 4443–4458.
- [4] D. Jiang, T. He, L. Ma, Z. Wang, *RSC Adv.* 4 (2014) 64936–64946.
- [5] P. Padmaja, P. Narayana Reddy, B.V. Subba Reddy, *Org. Biomol. Chem.* 18 (2020) 7514–7532.
- [6] C. Liu, W. Huang, J. Zhang, Z. Rao, Y. Gu, F. Jérôme, *Green Chem.* 23 (2021) 1447–1465.
- [7] S. Bondalapati, U.C. Reddy, P. Saha, A.K. Saikia, *Org. Biomol. Chem.* 9 (2011) 3428–3438.
- [8] B. Sarmah, G. Baishya, R.K. Baruah, *RSC Adv.* 4 (2014) 22387–22397.
- [9] I. Chneemann, I. Kajahn, B. Ohlendorf, H. Zinecker, A. Erhard, K. Nagel, J. Wiese, J.F. Imhoff Mayamycin, *J. Nat. Prod.* 73 (2010) 1309–1312.
- [10] S. Kelm, P. Madge, T. Islam, R. Bennett, H. Koliwer-Brandl, M. Waespy, M. Von Itzstein, T. Haselhorst, *Angew. Chem. Int. Ed.* 52 (2013) 3616–3620.
- [11] M. Chiba, Y. Ishikawa, R. Sakai, M. Oikawa, *ACS Comb. Sci.* 18 (2016) 399–404.
- [12] J. Huber, J. Wolfing, G. Schneider, I. Ocsóvski, M. Varga, I. Zupko, E. Mernyak, *Steroids* 102 (2015) 76–84.
- [13] C. Segovia, F. Fache, B. Pelotier, O. Piva, *ChemistrySelect* 4 (2019) 3191–3194.
- [14] N. Hazarika, B. Sarmah, M. Bordoloi, P. Phukan, G. Baishya, *Org. Biomol. Chem.* 15 (2017) 2003–2012.
- [15] B.L. Donnelly, L.D. Elliott, C.L. Willis, K.I. Booker-Milburn, *Angew. Chem., Int. Ed.* 58 (2019) 9095–9098.
- [16] B.V. Subba Reddy, K. Muralikrishna, J.S. Yadav, N. Jagdeesh Babu, K. Sirisha, A.V. S. Sarma, *Org. Biomol. Chem.* 13 (2015) 5532–5536.
- [17] T. Glachet, F. Fache, B. Pelotier, O. Piva, *Synthesis* 49 (2017) 5197–5202.
- [18] B.V.S. Reddy, S. Ghanty, *Synth. Commun.* 44 (2014) 2545–2554.
- [19] B.V. Subba Reddy, S. Ghanty, C. Kishore, B. Sridhar, *Tetrahedron Lett.* 55 (2014) 4298–4301.
- [20] N.P. Selvam, P.T. Perumal, *Can. J. Chem.* 87 (2009) 698–705.
- [21] J.S. Yadav, B.V. Subba Reddy, G.G.K.S. Narayana Kumar, G. MadhusudanReddy, *Tetrahedron Lett.* 48 (2007) 4903–4906.
- [22] P. Srinivasan, P.T. Perumal, S. Raja, *Indian J. Chem.* 50B (2011) 1083–1091.
- [23] O.L. Epstein, T. Ravis, A. Sakurai-Prins-Ritter, *J. Am. Chem. Soc.* 128 (2006) 16480–16481.
- [24] A. Behr, A.J. Vorholt, K.A. Ostrowski, T. Seidensticker, *Green. Chem.* 16 (2014) 982–1006.
- [25] T.M. Le, Z. Szakonyi, *Chem. Rec.* 22 (2022), e202100194.
- [26] E. Nazimova, A. Pavlova, O. Mikhailchenko, I. Il'ina, D. Korchagina, T. Tolstikova, K. Volcho, N. Salakhutdinov, *Med. Chem. Res.* 25 (2016) 1369–1383.
- [27] I.V. Ilyina, O.S. Patrusheva, V.V. Zarubaev, M.A. Misiurina, A.V. Slita, I. L. Esaulkova, D.V. Korchagina, Yu.V. Gatilov, S.S. Borisevich, K.P. Volcho, N. F. Salakhutdinov, *Bioorg. Med. Chem. Lett.* 31 (2021), 127677.
- [28] N.S. Li-Zhulanov, A.L. Zakharenko, A.A. Chepanova, J. Patel, A. Zafar, K.P. Volcho, N.F. Salakhutdinov, J. Reynisson, I.K.H. Leung, O.I. Lavrik, *Molecules* 23 (2018) 2468.
- [29] M. Zelińska-Blajet, P. Pietrusiak, J. Feder-Kubis, *Int. J. Mol. Sci.* 22 (2021) 4763.
- [30] Y.M. Mukhtar, K. Wang, R. Li, W. Deng, M. Adu-Frimpong, H. Zhang, K. Zhang, C. Gu, X. Xu, J. Yu, *RSC Adv.* 9 (2019) 19973–19982.
- [31] M. Zelińska-Blajet, J. Feder-Kubis, *Int. J. Mol. Sci.* 21 (2020) 7078.
- [32] A.S. Volobueva, O.I. Yarovaya, M.V. Kireeva, S.S. Borisevich, K.S. Kovaleva, I. Y. Mainagashev, Y.V. Gatilov, M.G. Ilyina, V.V. Zarubaev, N.F. Salakhutdinov, *Molecules* 26 (2021) 6794.
- [33] P.S. Sathe, J.D. Rajput, S.S. Gunaga, H.M. Patel, R.S. Bendre, *Res. Chem. Intermed.* 45 (2019) 5487–5498.
- [34] W.J. Huang, J.H. Liu, Q.M. She, J.Q. Zhong, G.E. Christidis, C.H. Zhou, *Catal. Rev.* (2021) 1–57, <https://doi.org/10.1080/01614940.2021.1995163>.
- [35] M. Massaro, R. Noto, S. Riel, *Catalysts* 12 (2022) 149.
- [36] R. Ramos, V.K. Abdelkader-Fernández, R. Matos, A.F. Peixoto, D.M. Fernandes, *Catalysts* 12 (2022) 207.
- [37] A.Yu. Sidorenko, N.S. Li-Zhulanov, P. Mäki-Arvela, T. Sandberg, A.V. Kravtsova, A. F. Peixoto, C. Freire, K.P. Volcho, N.F. Salakhutdinov, V.E. Agabekov, D.Yu. Murzin, *ChemCatChem* 12 (2020) 2605–2609.
- [38] N. Li-Zhulanov, P. Mäki-Arvela, M. Lalue, A.F. Peixoto, E. Kholkina, T. Sandberg, A. Aho, K. Volcho, N. Salakhutdinov, C. Freire, A.Yu. Sidorenko, D.Yu. Murzin, *Mol. Catal.* 478 (2019), 110569.
- [39] A.Yu. Sidorenko, Yu.M. Kurban, A.V. Kravtsova, I.V. Il'ina, N.S. Li-Zhulanov, D. V. Korchagina, J.E. Sánchez-Velandia, A. Aho, K.P. Volcho, N.F. Salakhutdinov, D. Yu. Murzin, V.E. Agabekov, *Appl. Catal. A Gen.* 629 (2022), 118395.
- [40] A.Yu. Sidorenko, A.V. Kravtsova, A. Aho, I. Heinmaa, J. Wana, H. Pazniak, K. P. Volcho, N.F. Salakhutdinov, D.Yu. Murzin, V.E. Agabekov, *J. Catal.* 374 (2019) 360–377.
- [41] A.Yu. Sidorenko, Yu.M. Kurban, I.V. Il'ina, N.S. Li-Zhulanov, D.V. Korchagina, O. V. Ardashov, J. Wärmä, K.P. Volcho, N.F. Salakhutdinov, D.Yu. Murzin, V. E. Agabekov, *Appl. Catal. A:Gen.* 618 (2021), 118144.
- [42] R. Barakov, N. Shcherban, P. Yaremov, I. Bezverkhyy, J. Čejka, M. Opanasenko, *Green. Chem.* 22 (2020) 6992–7002.
- [43] R. Barakov, N. Shcherban, O. Petrov, J. Lang, M. Shamzhy, M. Opanasenko, J. Čejka, *Inorg. Chem. Front.* 9 (2022) 1244–1257.
- [44] R.F. Cotta, R.A. Martins, K.A. da Silva Rocha, E.F. Kozhevnikova, I.V. Kozhevnikov, E.V. Gusevskaya, *Catal. Today* 381 (2021) 254–260.
- [45] L.J. Konwar, P. Mäki-Arvela, J.P. Mikkola, *Chem. Rev.* 119 (22) (2019) 11576–11630.
- [46] E. Lam, J.H. Luong, *ACS Catal.* 4 (2014) 3393–3410.
- [47] A.F. Peixoto, R. Ramos, M.M. Moreira, O.S.G. Soares, L.S. Ribeiro, M.F. Pereira, C. Delerue-Matos, C. Freire, *Fuel* 303 (2021), 121227.
- [48] J.H. Advani, A.S. Singh, H.K. Noor-ul, H.C. Bajaj, A.V. Biradar, *Appl. Catal. B Environ.* 268 (2020), 118456.
- [49] J. Tirado-Reves, W.J. Jorgensen, *Chem. Theory Comput.* 4 (2008) 297–306.
- [50] S. Grimme, J. Antony, S. Ehrlich, H. Krieg, *J. Chem. Phys.* 132 (2010), 154104.
- [51] W. Reckien, F. Janetzko, M.F. Peintinger, T. Bredow, *Comput. Chem.* 33 (2012) 2023–2031.
- [52] I. Muthuvel, B. Krishnakumar, M. Swaminathna, *Ind. J. Chem.* 51A (2012) 800–806.
- [53] M. Breugst, R. Grée, K.N. Houk, *J. Org. Chem.* 78 (2013) 9892–9897.
- [54] A.Yu. Sidorenko, Yu.M. Kurban, A. Aho, Zh.V. Ihnatovich, T.F. Kuznetsova, I. Heinmaa, D.Yu. Murzin, V.E. Agabekov, *Mol. Catal.* 499 (2021), 111306.
- [55] A.Yu. Sidorenko, A.V. Kravtsova, J. Wärmä, A. Aho, I. Heinmaa, I.V. Il'ina, O. V. Ardashov, K.P. Volcho, N.F. Salakhutdinov, D.Yu. Murzin, V.E. Agabekov, *Mol. Catal.* 453 (2018) 139–148.
- [56] X. Yang, Z. Liu, G. Wei, Y. Gu, H. Shi, *Chin. J. Catal.* 43 (2022) 1964–1990.
- [57] H. Haario, *ModEst, Modelling and Optimization Software*, Helsinki, 2011.
- [58] D.Yu. Murzin, T. Salmi, *Catalytic Chemistry and Engineering*, 2d edition., Elsevier, 2016, p. 740.